ehp ENVIRONMENTAL HEALTH PERSPECTIVES
http://www.ehponline.org

Synergistic and Antagonistic Mutation Responses of Human MCL-5 Cells to Mixtures of Benzo[a]pyrene and 2-Amino-1-Methyl-6-Phenylimidazo[4,5-b]pyridine: Dose-Related Variation in the Joint Effects of Common Dietary Carcinogens

Rhiannon David, Timothy Ebbels, and Nigel Gooderham

http://dx.doi.org/10.1289/ehp.1409557

Received: 4 December 2014
Accepted: 16 June 2015
Advance Publication: 19 June 2015

Editor's Note: An error was found in this article after acceptance. The correction is included before the original manuscript. The error will be corrected in the final version of the article.

Synergistic and Antagonistic Mutation Responses of Human MCL-5 Cells to Mixtures of Benzo[a]pyrene and 2-Amino-1-Methyl-6-Phenylimidazo[4,5-b]pyridine: Dose-Related Variation in the Joint Effects of Common Dietary Carcinogens

Rhiannon David, Timothy Ebbels, and Nigel Gooderham

DOI: 10.1289/ehp.1409557

Equation 4 in the Advance Publication was incorrect. The correct equation is shown below.

$$SEM = \sqrt{(\mathrm{SEM}_{\mathrm{G1G2}})^2 + (\mathrm{SEM}_{\mathrm{G1}})^2 + (\mathrm{SEM}_{\mathrm{G2}})^2 + \mathrm{C}}$$

Environ Health Perspect DOI: 10.1289/ehp.1409557
Advance Publication: Not Copyedited

Synergistic and Antagonistic Mutation Responses of Human MCL-5 Cells to Mixtures of Benzo[a]pyrene and 2-Amino-1-Methyl-6-Phenylimidazo[4,5-b]pyridine: Dose-Related Variation in the Joint Effects of Common Dietary Carcinogens

Rhiannon David[1,*], Timothy Ebbels[1], and Nigel Gooderham[1]

[1]Computational and Systems Medicine, Imperial College London, Sir Alexander Fleming Building, South Kensington Campus, London, SW7 2AZ, UK

Address correspondence to Nigel Gooderham, Computational and Systems Medicine, Imperial College London, Sir Alexander Fleming Building, South Kensington Campus, London, SW7 2AZ, UK. Telephone: 02075943188. E-mail: n.gooderham@imperial.ac.uk

*Current Address: Drug Safety and Metabolism, AstraZeneca, Darwin building, Milton Science Park, Cambridge, CB4 0WG, UK

Running title: Mutation responses to mixtures of BaP and PhIP

Acknowledgments: This work was supported by a grant from the Food Standards Agency UK (T01052).

Competing financial interests: The authors disclose no potential conflicts of interest.

Abstract

Background: Chemical carcinogens such as benzo[a]pyrene (BaP) and 2-amino-1-methyl-6-phenylimidazo[4,5-b]pyridine (PhIP) may contribute to the etiology of human diet-associated cancer. Individually, these are genotoxic, but the consequences of exposure to mixtures of these chemicals have not been systematically examined.

Objectives: To determine the mutagenic response to mixtures of BaP and PhIP at concentrations relevant to human exposure (mM to sub-nM).

Methods: Human MCL-5 cells (metabolically competent) were exposed to BaP or PhIP individually or in mixtures. Mutagenicity was assessed at the thymidine kinase (TK) locus, CYP1A activity and message determined by Ethoxyresorufin-*O*-deethylase (EROD) activity and Q-PCR respectively, and cell cycle measured by flow cytometry.

Results: Mixtures gave modified dose-responses compared to the individual chemicals; a remarkable increased mutant frequency (MF) at low concentration combinations (not mutagenic individually), and decreased MF at higher concentration combinations, compared to the calculated predicted additive MF of the individual chemicals. EROD activity and *CYP1A1* mRNA levels correlated with TK MF supporting involvement of the CYP1A family in mutation. Moreover, a cell cycle G2/M phase block was observed at high dose combinations, consistent with DNA damage sensing and repair.

Conclusions: Mixtures of these genotoxic chemicals produced mutation responses that differed from expectations for additive effects of the individual chemicals. The increase in MF for some combinations of chemicals at low concentrations that were not genotoxic for the individual chemicals, and the non-monotonic dose response, may be important for understanding the mutagenic potential of food and the etiology of diet-associated cancers.

Introduction

Consumption of red meat, is positively correlated with some human cancers and cooking meat produces heterocyclic amines (HCAs) and polycyclic aromatic hydrocarbons (PAHs) (Sinha et al. 2005). The HCA 2-amino-1-methyl-6-phenylimidazo[4,5-b]pyridine (PhIP) is bioavailable to humans consuming cooked meat (ingesting 0.1–15μg PhIP per day) (Felton et al. 2002) and a rodent carcinogen (Sugimura 1997), inducing cancer in the prostate, colon and mammary gland of rats (Crofts et al. 1997; Ito et al. 1991). PhIP is activated via *N*-hydroxylation catalysed by cytochromes P450 (CYP) 1A1 and 1A2, to DNA damaging species (Crofts et al. 1997; Zhao et al. 1994) forming promutagenic adducts at C8 of guanine, resulting in GC:TA transversions and deletions (Boyce et al. 2014; Lynch et al. 1998). Benzo[a]pyrene (BaP) is carcinogenic and generated by incomplete combustion of organic substances resulting in contamination of numerous foodstuffs (Lijinski and Shubik 1964). BaP is metabolised by CYP1A family to epoxide derivatives that form DNA adducts and result in mutation and tumours (IARC 2010). Through consumption of contaminated food, average human daily exposure to BaP is estimated at 1-500ng (IARC 2010). Experimental studies suggest a positive link between exposure to BaP and cancer in animals and in humans (Sinha et al. 2005).

Published assessment of genotoxic carcinogens, particularly dietary carcinogens, in mixtures is limited. Current approaches to mixtures risk assessment include whole-mixture and component-based methods (Agency for Toxic Substances and Disease Registry (ATSDR) 2004; US EPA 2000), with whole-mixture approaches preferred since they account for unidentified components and interactions between chemicals. However, the complexity and variability of mixtures makes this approach difficult, and component-based methods such as dose- or response-additivity are often used (Boobis et al. 2011; COT 2002; Lutz et al. 2005). Synergistic

effects from interactions between PAHs on DNA adduct levels have been reported (Staal et al. 2007; Tarantini et al. 2009; Tarantini et al. 2011) and prolonged activation of DNA damage signalling suggestive of persistent DNA damage by mixtures of PAHs has been observed (Jarvis et al. 2013; Mattsson et al. 2009; Niziolek-Kierecka et al. 2012), suggesting that current risk assessment strategies may underestimate risk. Contrasting studies showing antagonistic or additive effects from mixtures of PAHs (Courter et al. 2008; Mahadevan et al. 2007; Marston et al. 2001; Staal et al. 2008; White 2002) or heterocyclic aromatic amines (Dumont et al. 2010) have been published. Importantly, to our knowledge there is no information regarding mixtures of PAHs with HCAs at concentrations that are relevant to human exposure (μM to sub-nM with highest concentrations in GI microenvironments), which is important for the risk assessment of food-borne chemical carcinogens. Thus our aim was to determine mutagenic response to mixtures of BaP and PhIP at concentrations relevant to human exposure.

Methods

Materials

RPMI-1640 medium (with phenol red, without L-glutamine and histidine), heat-inactivated horse serum (HIHS), L-glutamine, penicillin/streptomycin, and hygromycin B from Life Technologies, Paisley, UK. All other chemicals were purchased from Sigma-Aldrich, Poole, UK.

Cell culture

MCL-5 is a human B lymphoblastoid cell that expresses constitutive CYP1A1 (Crespi et al. 1991) and stable expression of transfected CYP3A4, CYP2E1, CYP1A2, CYP2A6 and microsomal epoxide hydrolase (Crespi et al. 1991). Thus, this cell line can activate BaP and PhIP to DNA damaging species without the need for exogenous activation systems (S9 fraction).

Moreover, these cells are relevant for the human exposure route (the diet), as CYP1A1 is expressed in the GI tract (Paine et al. 2006). Cells were cultured in RPMI-1640 medium supplemented with 10% (v/v) HIHS, 2mM L-glutamine, 100units/ml penicillin, 100µg/ml streptomycin, 2mM histidinol and 200µg/ml hygromycin B, media called R10. Stocks were not cultured beyond 5 weeks (Johnson et al. 2010a; Johnson et al. 2010b).

HAT treatment of cells

To remove background mutants, MCL-5 cells were cultured for 3 days in R10 containing HAT (hypoxanthine, aminopterin, thymidine; Hybri-Max™), which is lethal to cells that harbour mutations at the TK locus (Busby Jr et al. 1994). Subsequently, cells were transferred to media containing HT (hypoxanthine, thymidine; Hybri-Max™) for 24h then mutant-depleted cultures were maintained for 4 days in normal media prior to freezing.

TK Forward Mutation Assay

Mutation assays used HAT treated cells (50ml at 4 x 10^5 cells/ml) with BaP or PhIP or binary mixtures to achieve final concentrations outlined in Table 1. Dimethylsulfoxide (DMSO; 0.1% v/v) was the negative control and ethyl methanesulfonate (EMS; 10µg/ml) the positive control for all experiments. Mutation data were considered acceptable provided the Relative Total Growth (RTG) and mutant frequency (MF) for both DMSO and EMS controls complied with historical data, and RTG additionally complied with OECD guidelines (data not shown) (OECD Guideline 476 1997). Published methodology (Clements 2000) with some optimizations was followed. Cells were treated for 24h in RPMI-1640 containing all supplements but reduced serum (5% (v/v) HIHS), at 37°C, 5% CO_2. Following treatment, the cellular concentration was adjusted to 4x10^5 cells/ml and subcultured daily for 2 further days to determine relative

suspension growth (RSG). On the third day cells were plated (10 cells/well in 2 x 96 well plates) for cloning efficiency (CE) and 20 000 cells/well in 3 x 96 well plates in trifluorothymidine (TFT; 4μg/ml) to determine thymidine kinase (TK) MF. Plates were incubated for 21 days to determine MF. RTG was calculated to estimate cytotoxicity and MF expressed as mutants/10^6 viable cells (Clements 2000).

***Ethoxyresorufin-O-deethylase* (EROD)**

Ethoxyresorufin-*O*-deethylase (EROD, indicator of CYP1A activity), was measured as conversion of 7-ethoxyresorufin (7-ER) to resorufin. Cell suspensions (10ml at 4 x 10^5 cells/ml) were treated with selected concentrations of BaP or PhIP, or combinations of BaP with PhIP, for 24h then 3x10^6 cells collected for EROD activity analysis by centrifugation (200x*g*, 5 minutes, RT), washed once in phenol red-free serum-free RPMI-1640 media (R0) and re-suspended in 1ml R0 media in 24 well plates, 8μM 7-ER added and incubated (90 minutes, 37°C). Fluorescence was measured at λexcitation 560nm and λemission 590nm every 10 minutes (POLARstar Galaxy, BMG Lab Technologies). Activity was expressed as pmol resorufin produced/min/10^6 cells using a resorufin standard curve.

Protein Determination

Cells (3x10^6) collected by centrifugation (450x*g*, 5 minutes, RT) were treated with RIPA buffer (Sigma) with Halt protease inhibitor cocktail (Life Technologies) for 30 minutes on ice. Lysate was clarified by centrifugation (8000xg, 10 minutes, 4°C), the supernatant collected and stored at -20°C. Lysate protein was determined using the BCA assay (Pierce, Thermo Scientific) following manufacturer's instructions.

Immunoblotting

Protein samples (20µg) were mixed with 5x loading buffer containing β-mercaptoethanol and adjusted to 25µl. Samples were boiled (95°C, 5 minutes), centrifuged (10,000x*g*, 5 minutes) and loaded onto a 10% SDS-polyacrylamide gel and electrophoresed (100V, 1.5 hours). Proteins were transferred to nitrocellulose membrane (150V, 400mA, 1.5 hours) and Ponceau S stain used to confirm transfer. The membrane was blocked (PBS-T 0.1% Tween 20, 5% milk powder) and then incubated with antibodies for MSH2 or MSH6 (Abcam, 1:1000 dilution, 4°C overnight). The membrane was incubated with a horseradish peroxidase-coupled goat anti-rabbit or goat anti-mouse secondary antibody (Abcam, 1:10000 dilution) for 1 hour at room temperature and protein bands detected using luminata forte Western HRP substrate (Merk-Millipore), visualized using the ChemiDoc XRS+ Molecular Imager System (BIO-RAD, California, USA). Blots were probed for β-actin as a loading control (primary antibody, 1 hour incubation, 1:200, Sigma; secondary antibody goat anti-mouse, 1 hour incubation, 1:10000, Abcam).

RNA Extraction and Quantitative RT-PCR (Q-PCR)

Following treatment with selected concentration combinations of BaP with PhIP, cells ($3x10^6$) were collected by centrifugation (200x*g*, 5 minutes, RT) and the pellet resuspended in 0.5ml Trizol (Invitrogen, Paisley, UK) for RNA extraction, quantified (Implen nanophotometer, GmbH, Munchen, Germany) and ratios A260/280 and A260/230 used to assess quality. To synthesise cDNA 1µl random primers was added to 500ng of RNA (final volume of 15µl with RNase/DNase-free dH_2O) and incubated (65°C, 5 minutes). The mixture was placed on ice before addition of 0.2mM dNTPs, 5µl 5x first strand buffer, 2µl 0.1mM DTT and 0.5µl Superscript II reverse transcriptase (Superscript II kit, Life Technologies). Samples were run on a thermocycler (25°C, 10 minutes; 42°C, 90 minutes; 70°C, 15 minutes). CYP1A1 cDNA was

amplified using Q-PCR. As an internal control, endogenous glyceraldehyde-3-phosphate dehydrogenase (GAPDH) cDNA from the same cellular extracts was also amplified. cDNA was amplified using Taqman Fast 2x Universal PCR master mix, No AmpErase UNG (Life Technologies) in triplicate. Q-PCR data were analysed using the ABI 7500 Sequence Detection System (Life Technologies) and comparative Ct Method (ΔC_T Method) (Livak and Schmittgen 2001). Calibration was based on the expression of GAPDH.

Flow cytometry analysis of cell cycle distribution

Cell cycle stage was determined using flow cytometry. MCL-5 cells were resuspended in 1ml 70% ethanol (in phosphate buffered saline; PBS) at -20°C. Cells were collected (450x*g*, 10 minutes, 4°C), washed once in PBS, resuspended in 200µl PBS containing propidium iodide (5µg/ml) and RNase A (0.1mg/ml), incubated (37°C, 30 minutes) and examined by flow cytometry (Fortessa II, Beckmann Coulter); cell cycle distribution was determined using FloJo software (Tree Star Inc., Oregon, US).

Statistical analysis of mutation data to determine synergy/antagonism

Median Effect Plot and Combination Index (CI)

Data were analysed by the method of Chou (2006) using background-corrected MF. Median effect plots of log(dose) vs log(fa/fu), where fa is the fraction affected (MF/1e6 viable cells) and fu is 1e6-fa, were drawn for individual chemicals to obtain the slope (m), the median effect dose (Dm, calculated as the antilog of the x intercept when y=0) and the Pearson correlation coefficient (r), which signify the shape of the dose-effect curve, the potency (IC_{50}), and the conformity of the data to the mass action law, respectively. From these, doses of individual chemicals alone required to produce the mixture effect were calculated using equation 1:

$$Dx = Dm[fa(mix)/1\text{-}fa(mix)]^{1/m} \quad [1]$$

The combination index (CI) was calculated using equation 2:

$$CI = D_1/Dx_1 + D_2/Dx_2 \quad [2]$$

where D_1 and D_2 are the concentrations of the individual chemicals used in the mixture and subscripts 1 and 2 refer to the two components of the mixture.

For the CI calculation, the value D was also calculated using equation 1. While D represents the dose of individual chemical used in the mixture, Chou (2006) states that *' dose and the effect are interchangeable since the dose (D) for any given effect (fa) can be determined if the values for Dm and m are known'*. Since Dm and m are obtained from the median effect plot, from which Dx values are also derived, it was noted that calculating D based on these values gave modified doses, thus we have adjusted D to reflect the median effect plot.

Synergism and antagonism are determined from CI and are subdivided into nearly additive (NDAd, 0.9-1.1), moderate synergism/antagonism (MS, 0.7-0.90/MA,1.1-1.45), synergism/antagonism (S,0.3-0.7/ A, 1.45-3.3), strong synergism/antagonism (SS, <0.3/ SA, >3.3) (Chou 2006).

Interaction factor (IF)

Data were also analysed using the interaction factor (IF), calculated with background-corrected MF following Danesi et al. (2012). The IFs were calculated using equation 3:

$$IF = G_1G_2 - G_1 - G_2 + C \quad [3]$$

where G_1G_2 is the MF obtained in treatment with the combination, G_1 and G_2 are the MF obtained in treatment with individual chemicals, and C is the MF obtained in control. A negative IF denotes antagonism, a positive IF denotes synergism and a zero IF denotes additivity.

The standard error of the mean (SEM) of IF was calculated as described by Danesi et al., (2012) using equation 4:

$$SEM = \sqrt{(\text{SEMG1G2})2 + (\text{SEMG1})2 + (\text{SEMG2})2 + \text{C}} \quad [4]$$

where SEM_{G1G2} is the SEM for the mixture.

Independent action (IA)

Concentration-response relationships of mixtures of compounds are predicted based on concentration-response data for individual mixture components, assuming additivity (Rajapakse et al. 2001). Synergism and antagonism can be defined as deviations from expected effects, with synergistic mixtures showing higher and antagonistic mixtures lower, responses than predicted. When predictions are met the combined response is additive (Berenbaum 1989). Independent action (IA) represents the situation where compounds act on different subsystems, possibly involving different sites and modes of action (Rajapakse et al. 2001). Since the chemicals used in this study have different mechanisms of action (both chemicals are activated by CYP1A1 and PhIP is additionally activated by CYP1A2 (Crofts et al. 1997; IARC 2010; Zhao et al. 1994), and while DNA damage from BaP is a result of ROS and epoxides, PhIP induces DNA damage via a nitrenium ion (IARC 2010; Singh et al. 2010)), IA was also used for determining expected response.

IA can be calculated using equation 5 as described by Berenbaum (1989):

$$E(da, db) = E(da) + E(db) – E(da)E(db) \quad [5]$$

where E(da, db) is the fractional effect of the mixture, and E(da) and E(db) is the fractional effect of individual chemicals. In this equation, fractional effect E is used as a substitute for probability of occurrence of an event, and fractional lack of effect (Berenbaum 1989). When applying this model, a maximal effect has to be defined (Rajapakse et al. 2001). In the current study, the fractional effect E is the MF, which is expressed as number of mutants per 1e6 viable cells, thus we assume the unit of assessment is the cell and maximal effect is 1e6 mutants per 1e6 cells.

IA was calculated using equation 6, based on that employed by Abendroth et al. (2011):

$$IA = E_1 + E_2 - (E_1E_2/10^6) \quad [6]$$

where IA is the predicted mixture percent response assuming additivity, E_1 is the observed percent response for chemical 1 alone, and E_2 is the observed percent response for chemical 2 alone.

Statistical analysis

Statistical significance was determined using a one way ANOVA with Dunnett's post-test. Statistical significance was defined as $P \leq 0.05$.

Results

TK forward mutation assay for individual chemicals

Concentrations of BaP and PhIP used were chosen to cover typical human dietary exposure ($<10^{-8}$M) (IARC 2010; Sinha et al. 2005) to high concentrations that induce a high mutant frequency (Felton et al. 2002; Yadollahi-Farsani et al. 1996). BaP produced a statistically significant increase in TK MF from $2.5x10^{-7}$ to 10^{-5}M (Figure 1A), while treatment of cells with PhIP required higher doses than BaP (Figure 1B). PhIP has been reported to be a poor mammalian cell

mutagen in *in vitro* assays (Knize et al. 2002; Yadollahi-Farsani et al. 1996) requiring doses in the 10^{-5}-10^{-4}M range, consistent with the present study.

Mutant frequency at TK locus for binary mixture

The observed TK MF differed from the expected additive response (based on addition of the MF of individual chemicals and the model of Independent Action; IA). Broadly, MF was increased at low concentration combinations and decreased at high concentration combinations compared to the response expected if MF for individual chemicals was additive. For example, a remarkable statistically significant increase in MF was observed for the combination 10^{-7}M BaP with 10^{-6}M PhIP (TK MF = 43.6 ± 7.0), whereas these concentrations alone did not significantly increase the MF (TK MF = 1.3 ± 1.2 and 5.6 ± 2.4, respectively) (Figure 1C; Table 1). In contrast, the MF observed for 10^{-5}M BaP in combination with 10^{-4}M PhIP (TK MF = 7.9 ±2.5) was considerably lower than anticipated given that these concentrations produced significant increases in MF individually (TK MF = 76.9 ± 10.5 and 7.9 ± 2.4, respectively) (Figure 1C; Table 1). The RTG for the different mixtures did not change significantly from the RTG observed when those concentrations were tested for the chemicals individually, suggesting no significant toxicity from the individual or combined treatments (Table 1).

Statistical analysis of the binary mixture data

Three methods of statistical determination of interaction were employed to assess whether combinations of BaP with PhIP were additive, synergistic or antagonistic. The Median Effect Equation derived from the mass action law principle (Chou 2006) allows quantitative determination of chemical interactions leading to biological responses. This has previously been employed for mixtures where a maximum effect is achievable, (e.g. enzyme inhibition) (Chou

and Talalay 1984), but has not, to our knowledge, been applied to mutation data. Here we define a theoretical maximum effect limit for mutation (i.e. 1e6 mutants per 1e6 cells). Practically, this assumption is not achievable as mutation at this frequency is incompatible with survival. An alternative method is to use the interaction factor (IF) (Schlesinger et al. 1992), recently applied to genotoxicity data in *Drosophila* (Danesi et al. 2012). Thirdly, response addition based on independent action (IA), which represents the situation where compounds act on different subsystems possibly involving different sites and modes of action (Rajapakse et al. 2001), was calculated for the mixtures. This determines outcome based on additivity, and synergism and antagonism can be defined as deviations from expected effects. Results from all three analyses show a synergistic interaction for the combination BaP 10^{-7}M with PhIP 10^{-6}M, with the difference between the observed and predicted joint effect statistically significant based on IA. In contrast, six combinations involving BaP $\geq 10^{-6}$M with doses of PhIP $\geq 10^{-6}$M were consistently categorized as antagonistic by all three methods, with statistically significant differences between the observed and predicted joint effects based on IA for five of the six combinations (Table 2).

Ethoxyresorufin-O-deethylase (EROD) activity

BaP and PhIP require metabolic activation to genotoxic products catalyzed by CYP1A. EROD (indicator of CYP1A activity) was measured in cells treated with BaP or PhIP individually, or BaP-PhIP mixtures. Results show induction of EROD at concentrations $\geq 10^{-7}$M BaP (Figure 2A) while induction was only observed with 10^{-8}M PhIP (Figure 2B). For the selected combinations, the results show induction of EROD activity for 10^{-7}M BaP with 10^{-6}M PhIP, $2.5x10^{-7}$M BaP with 10^{-6}M PhIP, and 10^{-6}M BaP with 10^{-6}M PhIP, with no induction for other combinations tested (Figure 2C). EROD activity for mixtures was found to be significantly correlated with TK MF ($P=<0.0001$, $R=0.78$; Figure 2D).

It should be noted that EROD activity cannot be measured at >10^{-5}M BaP as this is above the Km for CYP1A1 where BaP outcompetes 7-ER for CYP (Crofts et al., 1997).

CYP1A1 mRNA expression levels

Q-PCR for *CYP1A1* mRNA from cells treated with mixtures of BaP with PhIP showed significant increases (compared with control) for mixtures with BaP concentrations ≥10^{-7}M BaP combined with 10^{-6}M PhIP. However, at each BaP concentration ≥10^{-7}M, the increase in CYP1A1 expression diminished as the concentration of PhIP increased (e.g. for mixtures of 10^{-5}M BaP plus PhIP and 10^{-6}, 10^{-5}, and 10^{-4}M concentrations respectively) (Figure 2E). The *CYP1A1* mRNA levels significantly correlated with the TK MF profile (P=<0.0001, R=0.80; Figure 2F).

Cell cycle

To determine whether alterations in cell cycle play a role in the altered MF response observed following exposure to combinations of BaP with PhIP, cell cycle status was measured following a 24h treatment with selected combinations, and after a 24h and 48h recovery phase.

A significant decrease in the number of cells in S phase after 24h was observed for the two highest dose combinations (10^{-5}M BaP with either 5x10^{-5}M (P≤0.05) or 10^{-4}M PhIP (P≤0.01); Table 3). There was also a corresponding significant increase in the sub-G1 population, significant for all combinations except 10^{-9}M BaP with 10^{-9}M PhIP (Table 3) suggestive of apoptosis.

Following a 24h recovery period, significant increases in the number of cells in sub G1 were observed for combinations ≥10^{-7}M BaP with 10^{-6}M PhIP, suggestive of apoptosis, and a significant increase in the number of cells in G2/M phase was observed for 10^{-6}M BaP with

$5x10^{-5}$M PhIP, and 10^{-5}M BaP with either $5x10^{-5}$ or 10^{-4}M PhIP (Figure 3; Table 3). Accumulation of cells in G2/M phase occurs at concentration combinations where antagonistic effects were observed and may reflect a block in the cell cycle to allow DNA repair.

Following a 48h recovery period, a significant accumulation of cells in G1 phase was observed for combinations 10^{-6}M BaP with $5x10^{-5}$M PhIP and 10^{-5}M BaP with 10^{-4}M PhIP (Table 3). This pattern of cell cycle phase accumulation is indicative of a population of synchronized cells moving through the cycle after arrest release (Creton et al. 2005; Zhu et al. 2000).

Expression of mismatch repair proteins MSH2 and MSH6

PhIP has been linked with induction of G2 arrest and an increase in levels of MSH6/GTBP (Creton et al. 2005) to determine whether the reduced MF observed at some concentration combinations was associated with increased DNA repair, levels of mismatch repair proteins MSH2 and MSH6 (hMutSa complex) were measured.

Following treatment with selected mixtures of BaP and PhIP (10^{-7}M or 10^{-5}M BaP with either 10^{-6}M, $5x10^{-5}$M, or 10^{-4}M PhIP) MSH6 protein levels were apparently increased at concentration combinations with 10^{-5}M BaP compared to with 10^{-7}M BaP (although no combinations tested were statistically significantly different to the control), where antagonistic induction of TK MF was observed (e.g. 10^{-5}M BaP with 10^{-6}M PhIP) (Figure 4A and C). No change in the level of MSH2 was observed (Figure 4B and C).

Since PhIP has been linked with induction of G2 arrest and mismatch repair (Creton et al. 2005; Duc and Leong-Morgenthaler 2004), levels of MSH6 were measured following a 24h PhIP treatment. A dose-dependent increase in MSH6 protein was observed, although only

significantly induced at 10^{-4}M (Figure 4D), suggesting PhIP may be responsible for induction of MSH6 protein by the mixtures.

Discussion

Eating cooked red meat strongly correlates with diet-associated cancers and cooking leads to the formation of chemical carcinogens such as BaP and PhIP (Sinha et al. 2005). Many studies have investigated DNA damage caused by individual chemicals but few have examined the consequences of exposure to mixtures. The current study aimed to examine mixtures of food-borne genotoxic carcinogens BaP with PhIP at doses that are relevant to human exposure.

Results from the TK mutation assay show BaP induces a statistically significant increase in MF at concentrations $>10^{-7}$M while PhIP significantly increased MF at concentrations $\geq 5x10^{-5}$M. In V79 Chinese hamster cells, MF at the HPRT locus was more pronounced in response to PhIP (Yadollahi-Farsani et al. 1996) than TK MF in MCL-5 cells exposed to the same PhIP cocentrations in the present study. However V79 cells express a non-functional p53 protein (Chaung et al. 1997) and are more susceptible to mutation than MCL-5 cells, which have a functional p53 response (Guest and Parry 1999).

It is noteworthy that 10^{-7}M BaP and 10^{-6}M PhIP did not increase MF as individual exposures (Table 1), whereas in combination they induced a significant mutation response that was synergistic based on CI, IF or IA analyses (Table 2). A recent report using the micronucleus assay showed that binary mixtures of dissimilar acting chemicals at their no observed genotoxic effect levels induced a significant increase in micronuclei, supporting our findings (Johnson et al. 2012). In contrast, the combined effect for the combination of 10^{-5}M BaP with 10^{-4}M PhIP was significantly and substantially lower than predicted based on expectations for additive effects.

Both compounds require metabolic activation by CYP1A1 family (IARC 2010; Zhao et al. 1994). EROD activity significantly correlated with the trend for MF, suggesting that CYP1A is required for mutation. In support, *CYP1A1* mRNA levels strongly correlated with TK MF. The increase in expression and activity of CYP1A1 is expected since BaP induces CYP1A1 expression via Aryl hydrocarbon receptor (AhR) (Nebert et al. 1993). The correlation of CYP1A1 expression and activity with the observed TK MF suggests that increased activation of the chemicals may represent one reason for the observed synergism. The Km of BaP and PhIP for human CYP1A1 is 8.8μM and 5.1μM respectively and the Km of PhIP for human CYP1A2 is 79μM (Crofts et al. 1997; Schwarz et al. 2001). Thus for mixture combinations where MF synergy was observed, the BaP/PhIP concentrations are below the Km of CYP1A1 and 1A2 and the enzymes are working with maximum efficiency. Unexpectedly, there is less induction of *CYP1A1* mRNA and EROD as the concentration of PhIP in the mixture increases, in line with the lower TK MF observed at these concentration combinations. A possible explanation for lack of induction of CYP1A1 with increasing PhIP in the mixture is that PhIP is oestrogenic and can mediate gene transcription via oestrogen receptor (ER) (Lauber et al. 2004). Aryl hydrocarbon Receptor Nuclear Translator (ARNT) is recruited to oestrogen-responsive promoters in the presence of oestradiol (Swedenborg and Pongratz 2010), thus PhIP may be recruiting ARNT to ER, reducing its availability for AhR and CYP1A1 transcription and thus CYP1A activity. Although elevation of mRNA was observed for higher concentration combinations (PhIP with 10^{-5}M BaP), the observed increases in TK MF were less than additive. At these higher mixture concentrations, access for metabolic enzymes becomes competitive (based on the Km for BaP and PhIP), thus limiting formation of DNA damaging metabolites resulting in antagonism of MF. Another possible explanation reflects the cell cycle status of cells.

Analysis of cell cycle 24h after treatment with selected combinations revealed significant accumulation of cells in sub G1 and a block at G2/M, which was dose-dependent with increasing concentrations of PhIP. Combinations of 10^{-6}M BaP with $5x10^{-5}$M PhIP, or 10^{-5}M BaP with either $5x10^{-5}$M or 10^{-4}M PhIP showed a significant accumulation of cells in G2/M and an antagonistic effect on TK MF, suggesting that G2/M phase arrest may play a role in the low MF observed. While a significant induction of CYP1A1 expression was observed for these combinations, suggestive of increased activation of the chemicals and therefore increased DNA damage, activation of G2/M phase arrest may allow damage repair reducing MF towards baseline levels. Indeed, G2/M block was not observed 48h after treatment, suggesting that damage had been repaired. The temporal dependency of accumulation of cells at different stages of the cell cycle could reflect release of cells from the initial S phase block, synchronizing this cell population.

Arrest at G2/M has been reported for these chemicals individually; BaP (10^{-5}M) has been shown to induce G2/M phase arrest following a 48h treatment (Drukteinis et al. 2005) and activation of G2/M checkpoint has been reported 24h after PhIP treatment (Duc and Leong-Morgenthaler 2004). Moreover, a recent study showed that complex mixtures of PAHs activated checkpoint kinase 1 (Chk1) (Jarvis et al. 2013), which mediates G2/M phase arrest. G2/M arrest has been linked with mismatch repair for certain types of DNA damage (Aquilina et al. 1999; Duc and Leong-Morgenthaler 2004; Hawn et al. 1995) and involvement of GTBP/MSH6 in PhIP-induced mutagenesis has previously been reported, with levels of these proteins elevated following PhIP exposure (Creton et al. 2005). In the current study an apparent increase in the levels of MSH6 protein was observed following a 24h treatment with concentration combinations with 10^{-5}M BaP compared to with 10^{-7}M BaP . MSH6 forms the MutSα complex

with MSH2, and this heterodimer binds bulky adducts at the C8 position of guanine produced by aminofluorene (AF) and 2-acetyl-4-aminofluorene (AAF) (Li et al. 1996), and is believed to be involved in repair of this type of DNA damage. Since PhIP generates bulky adducts at the C8 position of guanine, it is hypothesised that mismatch repair proteins are also involved in recognizing dG-C8-PhIP adducts (Duc and Leong-Morgenthaler 2004); (Glaab et al. 2000). Induction of MSH6 protein supports induction of cell cycle arrest to repair DNA damage at high dose combinations. Interestingly, involvement of DNA repair in non-monotonic dose responses has been reported in relation to the HPRT assay (Jenkins et al. 2010) and more recently in reference to low dose no observed genotoxic effect levels (Thomas et al. 2013).

Conclusions

Co-exposure to BaP and PhIP produce mutation responses that differ considerably from those expected based on the IA model of additivity. Combining the measurably non-mutagenic dose of 10^{-7}M BaP with the non-mutagenic concentration of 10^{-6}M PhIP results in a significant increase in TK MF. This may be mediated by CYP1A enzymes since EROD activity and *CYP1A1* mRNA correlated with MF (Figure 2). However, it should be noted that the majority of tested mixtures led to antagonistic effects. The less than additive TK MF at high dose combinations implies that such combinations are less mutagenic. Our data suggest there is involvement of DNA repair, mediated via G2/M phase arrest, for combinations with 10^{-5}M BaP. We hypothesise that in BaP-PhIP mixtures, BaP is the dominant mutagen making greatest contribution to the mutation response. This is supported by the increase in *CYP1A1* mRNA levels, likely to be BaP-driven since PhIP is a weak inducer of CYP1A1 (Thomas et al. 2006).

The increase in MF at low concentration combinations may be of significance when considering the genotoxic potential of food. These concentrations are more relevant to human

exposure and as such our results may have implications for risk assessment, since when mixtures are analysed based on their components a general assumption is made that interaction effects at low dose levels either do not occur or are small enough to be insignificant to the risk estimate (US EPA 2000), and our data show possible non-monotonic dose responses. Future work looking at DNA adduct formation would help clarify this.

In interpreting our observations, however, the limitations of current *in vitro* mutation assays must be appreciated, and prominent is the metabolism contribution to these processes. Although the MCL-5 cell line used in the current study is competent for Phase I metabolism of BaP and PhIP, it has limited ability to perform the totality of metabolic reactions that are available in intact mammals. All such *in vitro* mutagenicity models have deficient Phase II metabolism and the majority require added Phase 1 capability (S9) which limits detoxication thereby biasing towards a positive mutation response. In this respect, our cell-based system is similar to other *in vitro* mutation assays and all are likely to over-represent mutation potential. Thus detection of MF in *in vitro* mammalian cell systems should be viewed as indicative of mutagenic potential and further investigation of the mixture concentrations tested in the current study is required *in vivo* to fully assess the impact of these data for human health and risk assessment.

References

Abendroth JA, Blankenship EE, Martin AR, Roeth FW. 2011. Joint action analysis utilizing concentration addition and independent action models. Weed Technol 25:436-446.

Agency for Toxic Substances and Disease Registry (ATSDR). 2004. Assessment of joint toxic action of chemical mixtures. Available: Http://www.Atsdr.Cdc.Gov/interactionprofiles/ipga.Html [accessed 06/06/2015].

Aquilina G, Crescenzi M, Bignami M. 1999. Mismatch repair, g(2)/m cell cycle arrest and lethality after DNA damage. Carcinogenesis 20:2317-2326.

Berenbaum MC. 1989. What is synergy? Pharmacological Reviews 41:93-141.

Boobis A, Budinsky R, Collie S, Crofton K, Embry M, Felter S, et al. 2011. Critical analysis of literature on low-dose synergy for use in screening chemical mixtures for risk assessment. Critical reviews in toxicology 41:369-383.

Boyce A, David RM, Gooderham NJ. 2014. The mutagenic effects of 2-amino-1-methyl-6-phenylimidazo[4,5-b] pyridine in muta (tm) mouse colon is attenuated by resveratrol. Toxicol Res-Uk 3:197-204.

Busby Jr WF, Penman BW, Crespi CL. 1994. Human cell mutagenicity of mono- and dinitropyrenes in metabolically competent mcl-5 cells. Mutation Research/Genetic Toxicology 322:233-242.

Chaung W, Mi LJ, Boorstein RJ. 1997. The p53 status of chinese hamster v79 cells frequently used for studies on DNA damage and DNA repair. Nucleic acids research 25:992-994.

Chou, Talalay. 1984. Quantitative analysis of dose-effect relationships: The combined effects of multiple drugs or enzyme inhibitors. Advances in Enzyme Regulation 22:27-55.

Chou T-C. 2006. Theoretical basis, experimental design, and computerized simulation of synergism and antagonism in drug combination studies. Pharmacological Reviews 58:621-681.

Clements J. 2000. The mouse lymphoma assay. Mutat Res-Fund Mol M 455:97-110.

COT CoT. 2002. Risk assessment of mixtures of pesticides and similar substances. Committees on: Toxicity, mutagenicity, carcinogenicity of chemicals in food, consumer products and the environment.1-298.

Courter LA, Luch A, Musafia-Jeknic T, Arlt VM, Fischer K, Bildfell R, et al. 2008. The influence of diesel exhaust on polycyclic aromatic hydrocarbon-induced DNA damage, gene expression, and tumor initiation in sencar mice in vivo. Cancer Lett 265:135-147.

Crespi CL, Gonzalez FJ, Steimel DT, Turner TR, Gelboin HV, Penman BW, et al. 1991. A metabolically competent human cell line expressing five cdnas encoding procarcinogen-activating enzymes: Application to mutagenicity testing. Chemical Research in Toxicology 4:566-572.

Creton S, Zhu H, Gooderham NJ. 2005. A mechanistic basis for the role of cycle arrest in the genetic toxicology of the dietary carcinogen 2-amino-1-methyl-6-phenylimidazo[4,5-b]pyridine (phip). Toxicol Sci 84:335-343.

Crofts FG, Strickland PT, Hayes CL, Sutter TR. 1997. Metabolism of 2-amino-1-methyl-6-phenylimidazo[4,5-b]pyridine (phip) by human cytochrome p4501b1. Carcinogenesis 18:1793-1798.

Danesi CC, Dihl RR, Bellagamba BC, de Andrade HH, Cunha KS, Guimaraes NN, et al. 2012. Genotoxicity testing of combined treatment with cisplatin, bleomycin, and 5-fluorouracil in somatic cells of drosophila melanogaster. Mutat Res 747:228-233.

Drukteinis JS, Medrano T, Ablordeppey EA, Kitzman JM, Shiverick KT. 2005. Benzo[a]pyrene, but not 2,3,7,8-tcdd, induces g2/m cell cycle arrest, p21cip1 and p53 phosphorylation in human choriocarcinoma jeg-3 cells: A distinct signaling pathway. Placenta 26 Suppl A:S87-95.

Duc R, Leong-Morgenthaler PM. 2004. Role of p53 and mismatch repair in phip-induced perturbations of the cell cycle. Journal of chromatography B, Analytical technologies in the biomedical and life sciences 802:183-187.

Dumont J, Josse R, Lambert C, Antherieu S, Le Hegarat L, Aninat C, et al. 2010. Differential toxicity of heterocyclic aromatic amines and their mixture in metabolically competent heparg cells. Toxicol Appl Pharmacol 245:256-263.

Felton JS, Knize MG, Salmon CP, Malfatti MA, Kulp KS. 2002. Human exposure to heterocyclic amine food mutagens/carcinogens: Relevance to breast cancer. Environ Mol Mutagen 39:112-118.

Glaab WE, Kort KL, Skopek TR. 2000. Specificity of mutations induced by the food-associated heterocyclic amine 2-amino-1-methyl-6-phenylimidazo-[4,5-b]-pyridine in colon cancer cell lines defective in mismatch repair. Cancer research 60:4921-4925.

Guest RD, Parry JM. 1999. P53 integrity in the genetically engineered mammalian cell lines ahh-1 and mcl-5. Mutat Res 423:39-46.

Hawn MT, Umar A, Carethers JM, Marra G, Kunkel TA, Boland CR, et al. 1995. Evidence for a connection between the mismatch repair system and the g2 cell cycle checkpoint. Cancer research 55:3721-3725.

IARC. 2010. Iarc monographs on the evaluation of carcinogenic risks to humans, volume 92, some non-heterocyclic polycyclic aromatic hydrocarbons and some related exposures. Available: Http://monographs.Iarc.Fr/eng/monographs/vol92/mono92.Pdf [accessed 08/06/2015]. Vol. 92. Lyon, France.

Ito N, Hasegawa R, Sano M, Tamano S, Esumi H, Takayama S, et al. 1991. A new colon and mammary carcinogen in cooked food, 2-amino-1-methyl-6-phenylimidazo[4,5-b]pyridine (phip). Carcinogenesis 12:1503-1506.

Jarvis IW, Bergvall C, Bottai M, Westerholm R, Stenius U, Dreij K. 2013. Persistent activation of DNA damage signaling in response to complex mixtures of pahs in air particulate matter. Toxicol Appl Pharmacol 266:408-418.

Jenkins GJ, Zair Z, Johnson GE, Doak SH. 2010. Genotoxic thresholds, DNA repair, and susceptibility in human populations. Toxicology 278:305-310.

Johnson GE, Quick EL, Parry EM, Parry JM. 2010a. Metabolic influences for mutation induction curves after exposure to sudan-1 and para red. Mutagenesis 25:327-333.

Johnson GE, Quick EL, Parry JM. 2010b. T01038: The evaluation of the genotoxicity and concentration-response relationships of the azo dyes sudan 1 and para red. Food Standards Agency.

Johnson GE, Zair Z, Bodger OG, Lewis PD, Rees BJ, Verma JR, et al. 2012. Investigating mechanisms for non-linear genotoxic responses, and analysing their effects in binary combination. Genes and Environment 34:179-185.

Knize MG, Kulp KS, Salmon CP, Keating GA, Felton JS. 2002. Factors affecting human heterocyclic amine intake and the metabolism of phip. Mutat Res 506-507:153-162.

Lauber SN, Ali S, Gooderham NJ. 2004. The cooked food derived carcinogen 2-amino-1-methyl-6-phenylimidazo[4,5-b] pyridine is a potent oestrogen: A mechanistic basis for its tissue-specific carcinogenicity. Carcinogenesis 25:2509-2517.

Li GM, Wang H, Romano LJ. 1996. Human mutsalpha specifically binds to DNA containing aminofluorene and acetylaminofluorene adducts. The Journal of biological chemistry 271:24084-24088.

Lijinski W, Shubik P. 1964. Benzoapyrene and other polynuclear hydrocarbons in charcoal-broiled meat. Science 145:53-55.

Livak KJ, Schmittgen TD. 2001. Analysis of relative gene expression data using real-time quantitative pcr and the 2(-delta delta c(t)) method. Methods 25:402-408.

Lutz WK, Tiedge O, Lutz RW, Stopper H. 2005. Different types of combination effects for the induction of micronuclei in mouse lymphoma cells by binary mixtures of the genotoxic agents mms, mnu, and genistein. Toxicological sciences : an official journal of the Society of Toxicology 86:318-323.

Lynch AM, Gooderham NJ, Davies DS, Boobis AR. 1998. Genetic analysis of phip intestinal mutations in mutamouse. Mutagenesis 13:601-605.

Mahadevan B, Marston CP, Luch A, Dashwood WM, Brooks E, Pereira C, et al. 2007. Competitive inhibition of carcinogen-activating cyp1a1 and cyp1b1 enzymes by a standardized complex mixture of pah extracted from coal tar. International Journal of Cancer 120:1161-1168.

Marston CP, Pereira C, Ferguson J, Fischer K, Hedstrom O, Dashwood WM, et al. 2001. Effect of a complex environmental mixture from coal tar containing polycyclic aromatic hydrocarbons (pah) on the tumor initiation, pah-DNA binding and metabolic activation of carcinogenic pah in mouse epidermis. Carcinogenesis 22:1077-1086.

Mattsson A, Lundstedt S, Stenius U. 2009. Exposure of hepg2 cells to low levels of pah-containing extracts from contaminated soils results in unpredictable genotoxic stress responses. Environ Mol Mutagen 50:337-348.

Nebert DW, Puga A, Vasiliou V. 1993. Role of the ah receptor and the dioxin-inducible [ah] gene battery in toxicity, cancer, and signal transductiona. Annals of the New York Academy of Sciences 685:624-640.

Niziolek-Kierecka M, Dreij K, Lundstedt S, Stenius U. 2012. Gammah2ax, pchk1, and wip1 as potential markers of persistent DNA damage derived from dibenzo[a,l]pyrene and pah-containing extracts from contaminated soils. Chem Res Toxicol 25:862-872.

OECD Guideline 476. 1997. In vitro mammalian cell gene mutation test.

Paine MF, Hart HL, Ludington SS, Haining RL, Rettie AE, Zeldin DC. 2006. The human intestinal cytochrome p450 “pie”. Drug Metabolism and Disposition 34:880-886.

Rajapakse N, Ong D, Kortenkamp A. 2001. Defining the impact of weakly estrogenic chemicals on the action of steroidal estrogens. Toxicol Sci 60:296-304.

Schlesinger RB, Zelikoff JT, Chen LC, Kinney PL. 1992. Assessment of toxicologic interactions resulting from acute inhalation exposure to sulfuric acid and ozone mixtures. Toxicol Appl Pharmacol 115:183-190.

Schwarz D, Kisselev P, Cascorbi I, Schunck WH, Roots I. 2001. Differential metabolism of benzo[a]pyrene and benzo[a]pyrene-7,8-dihydrodiol by human cyp1a1 variants. Carcinogenesis 22:453-459.

Singh R, Arlt VM, Henderson CJ, Phillips DH, Farmer PB, Costa GGd. 2010. Detection and quantitation of n-(deoxyguanosin-8-yl)-2-amino-1-methyl-6-phenylimidazo[4,5-b]pyridine adducts in DNA using online column-switching liquid chromatography tandem mass spectrometry. Journal of Chromatography B 878:2155-2162.

Sinha R, Kulldorff M, Gunter MJ, Strickland P, Rothman N. 2005. Dietary benzo[a]pyrene intake and risk of colorectal adenoma. Cancer Epidemiol Biomarkers Prev 14:2030-2034.

Staal YC, Hebels DG, van Herwijnen MH, Gottschalk RW, van Schooten FJ, van Delft JH. 2007. Binary pah mixtures cause additive or antagonistic effects on gene expression but synergistic effects on DNA adduct formation. Carcinogenesis 28:2632-2640.

Staal YC, Pushparajah DS, van Herwijnen MH, Gottschalk RW, Maas LM, Ioannides C, et al. 2008. Interactions between polycyclic aromatic hydrocarbons in binary mixtures: Effects on gene expression and DNA adduct formation in precision-cut rat liver slices. Mutagenesis 23:491-499.

Sugimura T. 1997. Overview of carcinogenic heterocyclic amines. Mutation Research/Fundamental and Molecular Mechanisms of Mutagenesis 376:211 - 219.

Swedenborg E, Pongratz I. 2010. Ahr and arnt modulate er signaling. Toxicology 268:132-138.

Tarantini A, Maitre A, Lefebvre E, Marques M, Marie C, Ravanat JL, et al. 2009. Relative contribution of DNA strand breaks and DNA adducts to the genotoxicity of benzo[a]pyrene as a pure compound and in complex mixtures. Mutat Res 671:67-75.

Tarantini A, Maitre A, Lefebvre E, Marques M, Rajhi A, Douki T. 2011. Polycyclic aromatic hydrocarbons in binary mixtures modulate the efficiency of benzo[a]pyrene to form DNA adducts in human cells. Toxicology 279:36-44.

Thomas AD, Jenkins GJ, Kaina B, Bodger OG, Tomaszowski KH, Lewis PD, et al. 2013. Influence of DNA repair on nonlinear dose-responses for mutation. Toxicological sciences : an official journal of the Society of Toxicology 132:87-95.

Thomas RD, Green MR, Wilson C, Weckle AL, Duanmu Z, Kocarek TA, et al. 2006. Cytochrome p450 expression and metabolic activation of cooked food mutagen 2-amino-1-

methyl-6-phenylimidazo[4,5-b]pyridine (phip) in mcf10a breast epithelial cells. Chem Biol Interact 160:204-216.

US EPA. 2000. Supplementary guidance for conducting health risk assessment of chemical mixtures. Epa/630/r-00/002. Washington, dc: Risk assessment forum.

White PA. 2002. The genotoxicity of priority polycyclic aromatic hydrocarbons in complex mixtures. Mutat Res 515:85-98.

Yadollahi-Farsani M, Gooderham NJ, Davies DS, Boobis AR. 1996. Mutational spectra of the dietary carcinogen 2-amino-1-methyl-6- phenylimidazo[4,5-b]pyridine(phip) at the chinese hamsters hprt locus. Carcinogenesis 17:617-624.

Zhao K, Murray S, Davies DS, Boobis AR, Gooderham NJ. 1994. Metabolism of the food derived mutagen and carcinogen 2-amino-1-methyl-6-phenylimidazo(4,5-b)pyridine (phip) by human liver microsomes. Carcinogenesis 15:1285-1288.

Zhu H, Boobis AR, Gooderham NJ. 2000. The food-derived carcinogen 2-amino-1-methyl-6-phenylimidazo[4,5-b]pyridine activates s-phase checkpoint and apoptosis, and induces gene mutation in human lymphoblastoid tk6 cells. Cancer research 60:1283-1289.

Table 1. Relative Total Growth (RTG) and background-corrected mutation frequency (MF/1e6 viable cells) at the thymidine kinase (TK) locus following treatment with different concentrations of BaP and PhIP alone, or in selected combinations.

Treatment and Concentration (M)	RTG[a]	TK MF[b]
BaP		0.1± 1.3
10^{-10}	98.7± 0.7	0.1± 1.5
10^{-9}	95.1± 3.8	0.1± 1.8
10^{-8}	87.6± 5.9	1.3± 1.2
10^{-7}	85.6± 6.1	30.1**± 4.3
$2.5x10^{-7}$	85.6± 7.9	44.5***± 4.7
$7.5x10^{-7}$	74.1± 1.4	46.5***± 6.9
10^{-6}	74.2± 4.0	54.4***± 3.6
$2.5x10^{-6}$	85.9± 6.5	61.4***± 8.5
$7.5x10^{-6}$	64.4± 0.4	76.9***± 10.5
10^{-5}	56.4± 7.7	0.1± 1.3
PhIP		
10^{-9}	98.0± 3.9	0.7± 0.4
10^{-8}	113.2± 3.2	0.1± 1.3
10^{-7}	112.6± 6.8	5.6± 2.4
10^{-6}	114.2± 5.9	2.1± 1.6
10^{-5}	103.9± 2.9	5.1± 1.5
$5x10^{-5}$	89.2± 4.9	7.0**± 1.6
$7.5x10^{-5}$	78.6± 4.7	8.8*± 1.2
10^{-4}	83.0± 5.4	7.9**± 2.4
BaP+PhIP		
10^{-9}M+10^{-9}	109.8± 8.6	2.47± 2.13
10^{-7}M+10^{-6}	95.2± 7.8	43.6***± 11.38
10^{-7}M+$5x10^{-5}$	113.2± 12.2	0.1± 4.72
10^{-7}M+10^{-4}	89.4± 9.4	4.28± 2.81
$2.5x10^{-7}$M+10^{-6}	117.5± 8.8	56.81***± 10.68
10^{-6}M+10^{-6}	118.2± 1.2	39.71*± 4.56
10^{-6}M+$5x10^{-5}$	60.1± 8.2	17.5*± 4.17
10^{-6}M+10^{-4}	113.7± 13.3	2.93± 3.14
10^{-5}M+10^{-6}	48.3± 3.4	41.1***± 5.22
10^{-5}M+$5x10^{-5}$	100.9± 7.4	16.85*± 5.28
10^{-5}M+10^{-4}	81.6± 12.5	7.92± 2.49

[a]RTG values are % means ± Standard Error of the Mean (SEM), n=3-12. [b]Data are presented as background corrected means ± Standard Error of the Mean (SEM), n=3-12; DMSO negative control average range 4.9-18.6 and EMS positive control average range 74.6 – 125.5 MF/1e6 viable cells; Historical controls: TK: DMSO: 13.3±9.4 and EMS (positive control): 99.4±40.4 MF/1e6 viable cells ± standard deviation.

Significance compared to the DMSO control calculated using one-way ANOVA with Dunnett's post-test (* P≤0.05, ** P≤0.01, *** P≤0.001).

Table 2. Analysis of the mutation frequency data at the TK locus for BaP and PhIP in binary mixture by the Median Effect equation and the Combination Index Theorum (CI), Interaction Factor (IF) or Independent Action (IA).

BaP + PhIP[a]	fa[b]	CI[c]	Mechanism (CI)[d]	IF ± SEM[e]	Mechanism (IF)[e]	Predicted MF with IA[f]	Mechanism (IA)[g]
$10^{-9} + 10^{-9}$	2.47 ± 2.13	0.02	sS	1.64 ± 3.42	NDAd	0.83	NDAd
$10^{-7} + 10^{-6}$	43.60 ± 11.38	0.007	sS	40.25 ± 7.61	S	3.35***	S
$10^{-7} + 5x10^{-5}$	0.10 ± 4.72	$3.83x10^{6}$	sA	-8.15 ± 4.53	A	8.25	A
$10^{-7} + 10^{-4}$	4.28 ± 2.81	9.02	sA	-4.89 ± 4.35	NDAd	9.18	NDAd
$2.5x10^{-7} + 10^{-6}$	56.81 ± 10.68	0.29	sS	31.44 ± 11.83	S	32.18*	S
$10^{-6} + 10^{-6}$	39.71 ± 4.56	1.25	mA	-8.81 ± 8.74	A	48.52	A
$10^{-6} + 5x10^{-5}$	17.50 ± 4.17	3.99	sA	-35.92 ± 8.55	A	53.42***	A
$10^{-6} + 10-^{4}$	2.93 ± 3.14	83.33	sA	-51.42 ± 8.29	A	54.35***	A
$10-^{5} + 10^{-6}$	41.10 ± 5.22	2.42	A	-37.92 ± 12.05	A	79.02***	A
$10^{-5} + 5x10^{-5}$	16.85 ± 5.28	8.52	sA	-67.07 ± 12.07	A	83.92***	A
$10^{-5} + 10^{-4}$	7.92 ± 2.49	25.54	sA	-76.93 ± 11.28	A	84.85***	A

[a] Molar concentration (BaP is shown first); [b]Fraction affected (fa) is background corrected observed mutation frequency for the combinations/1e6 viable cells±SEM; [c]Combination Index (CI)=$(D_1/Dx_1)+(D_2/Dx^2)$; D_1, D_2 are the concentrations used in the mixture and Dx_1, Dx_2 are the concentrations of chemical alone to achieve the mixture effect; [d]Synergism and antagonism are subdivided into nearly additive (NAd, 0.9-1.1), moderate synergism/antagonism (mS, 0.7-0.90/mA,1.1-1.45), synergism/antagonism (S,0.3-0.7/ A, 1.45-3.3), strong synergism/antagonism (sS, <0.1-0.3/ sA, 3.3->10), (17); [e]Interaction factor (IF)=$G_1G_2-G_1-G_2+C$ ± SEM. A negative IF=antagonism (A), positive IF=synergism (S), 0=not different from additive (NDAd); [f]Independent Action (IA)=$MF_1+MF_2-[(MF_1MF_2)/10^6]$; MF_1 and MF_2 = individual MF, MF_1MF_2 = product of individual MFs.; [g]Mechanism deduced by comparison of predicted MF to the actual MF (fraction affected); Synergism (S), Antagonism (A), Not different from additive (NDAd). Observed and predicted MF response compared using a t test with Bonferroni multiple comparisons test (* P≤0.05; *** P≤0.001). Variance surrounding the expected MF was assumed to equal the variance for the observed data (Abendroth et al. 2011).

Table 3. Effects of selected combinations of BaP with PhIP on cell cycle distribution assessed by flow cytometry.

BaP and PhIP (M)	Sub G1 (24h)	G1 (24h)	S (24h)	G2/M (24h)	Sub G1 (24h post)	G1 (24h post)	S (24h post)	G2/M (24h post)	Sub G1 (48h post)	G1 (48h post)	S (48h post)	G2/M (48h post)
DMSO	4.99±1.30	34.30±2.05	21.93±1.70	24.30±1.31	0.97±0.36	36.20±0.83	30.97±1.68	21.80±0.81	0.11±0.24	43.97±0.91	21.23±0.52	23.00±0.70
$10^{-9}+10^{-9}$	4.92±0.77	34.77±1.57	19.47±0.59	26.17±0.97	1.27±0.20	35.10±0.46	31.47±1.91	22.90±1.87	1.08±0.39	42.93±1.02	19.77±1.29	22.37±1.23
$10^{-7}+10^{-6}$	4.72±0.51	35.73±1.34	22.87±0.98	23.80±0.72	2.38*±0.07	37.07±0.90	28.60±2.7	24.97±1.12	1.30±0.52	40.97±0.94	20.80±0.45	23.83±0.99
$2.5x10^{-7}+10^{-6}$	6.65±1.12	33.93±1.77	22.80±1.27	23.00±1.18	2.99***±0.50	36.30±0.90	26.97±1.36	27.07±1.30	1.46±0.24	40.00±2.48	20.77±2.00	24.37±0.43
$10^{-6}+5x10^{-5}$	7.34±1.03	34.30±1.05	18.07±1.19	25.77±0.10	2.45*±0.27	33.50±0.62	28.80±1.03	28.40*±0.40	1.59±0.90	36.60*±2.36	22.27±1.00	25.37±0.88
$10-^{5}+10^{-6}$	7.41±1.08	33.90±0.67	22.97±1.74	22.57±0.55	3.84***±0.16	32.43±0.58	31.27±2.07	26.70±2.31	6.08±1.31	37.93±1.61	21.57±4.53	24.23±1.51
$10^{-5}+5x10^{-5}$	8.74±1.04	34.47±0.73	15.23*±0.55	25.93±0.53	3.67***±0.25	33.60±1.06	28.80±2.45	29.73**±1.79	2.10±0.17	40.23±2.47	22.57±1.18	24.33±0.07
$10^{-5}+10^{-4}$	13.00**±2.40	39.73±2.31	14.07**±1.24	22.13±0.44	3.38***±0.29	32.83±1.07	29.57±1.04	30.73***±0.77	1.89±1.08	34.77**±1.56	26.03±0.49	23.93±1.77

Data are presented as the percentage of cells in each phase of the cell cycle ± SEM, n=3.

MCL-5 cells were treated for 24 h, as indicated, then harvested, or left in fresh media for a further 24 h (24h post) or 48 h (48h post) after treatment.

Dimethylsulfoxide (DMSO) was used as a negative control.

Significance compared to the negative control (DMSO) was calculated using one-way ANOVA with Dunnett's post-test (* $P \leq 0.05$, ** $P \leq 0.01$, *** $P \leq 0.001$).

Figure Legends

Figure 1. Effect of BaP, PhIP or BaP/PhIP mixtures on mutant frequency (MF) at the TK locus. Background corrected MF at TK locus following 24h treatment with (A) BaP, (B) PhIP or (C) BaP/PhIP mixtures; in (C) open bars are predicted MF based on additivity and solid bars are actual MF. DMSO negative control average range 4.9-18.6 and EMS positive control average range 74.6 – 125.5 MF/1e6 viable cells; Historical controls: TK: DMSO: 13.3±9.4 and EMS (positive control): 99.4±40.4 MF/1e6 viable cells ± standard deviation; Data are means ± SEM, n=3-12 independent cultures. Significance compared to DMSO control (one-way ANOVA with Dunnett's post-test; * P≤0.05, ** P≤0.01, *** P≤0.001).

Figure 2. Effect of BaP and PhIP mixtures on CYP1A activity and CYP1A1 expression. Ethoxyresorufin-*O*-deethylase (EROD) activity following 24h treatment with (A) BaP, (B) PhIP, or (C) combinations of BaP (concentration indicated first) and PhIP. (D) *CYP1A1* mRNA levels (Q-PCR, normalised to GAPDH) following 24h treatment with combinations of BaP and PhIP. Correlation of mixture TK MF with (E) mixture EROD or (F) mixture *CYP1A1* mRNA levels. For all mixtures, the concentration of BaP is stated first. Data are means ± SEM, n=3. Significance compared to the DMSO control (one-way ANOVA with Dunnett's post-test; * P≤0.05, ** P≤0.01, *** P≤0.001).

Figure 3. Effect of mixtures of BaP and PhIP on cell cycle. Percentage of cells in each phase of the cell cycle following a 24h treatment with selected combinations of BaP with PhIP or dimethylsulfoxide (DMSO) as the negative control with a subsequent 24h recovery period assessed by flow cytometry.

Figure 4. Effect of mixtures of BaP and PhIP, or PhIP alone, on mismatch repair proteins. The effect of a 24h treatment with selected concentration combinations of BaP (stated first) with PhIP on the expression of (A) MSH6 or (B) MSH2. (C) Representative Immunoblots showing the abundance of MSH6 and MSH2 proteins. (D) The effect of a 24h treatment with selected concentrations of PhIP on MSH6 protein expression. The intensity of each protein in DMSO-treated cells was used as a reference after correcting for loading (β-actin). Data are presented as mean ± SEM, n=3. Significance compared to the DMSO control calculated using one-way ANOVA with Dunnett's post-test (* P≤0.05).

Environ Health Perspect DOI: 10.1289/ehp.1409557
Advance Publication: Not Copyedited

Figure 1.

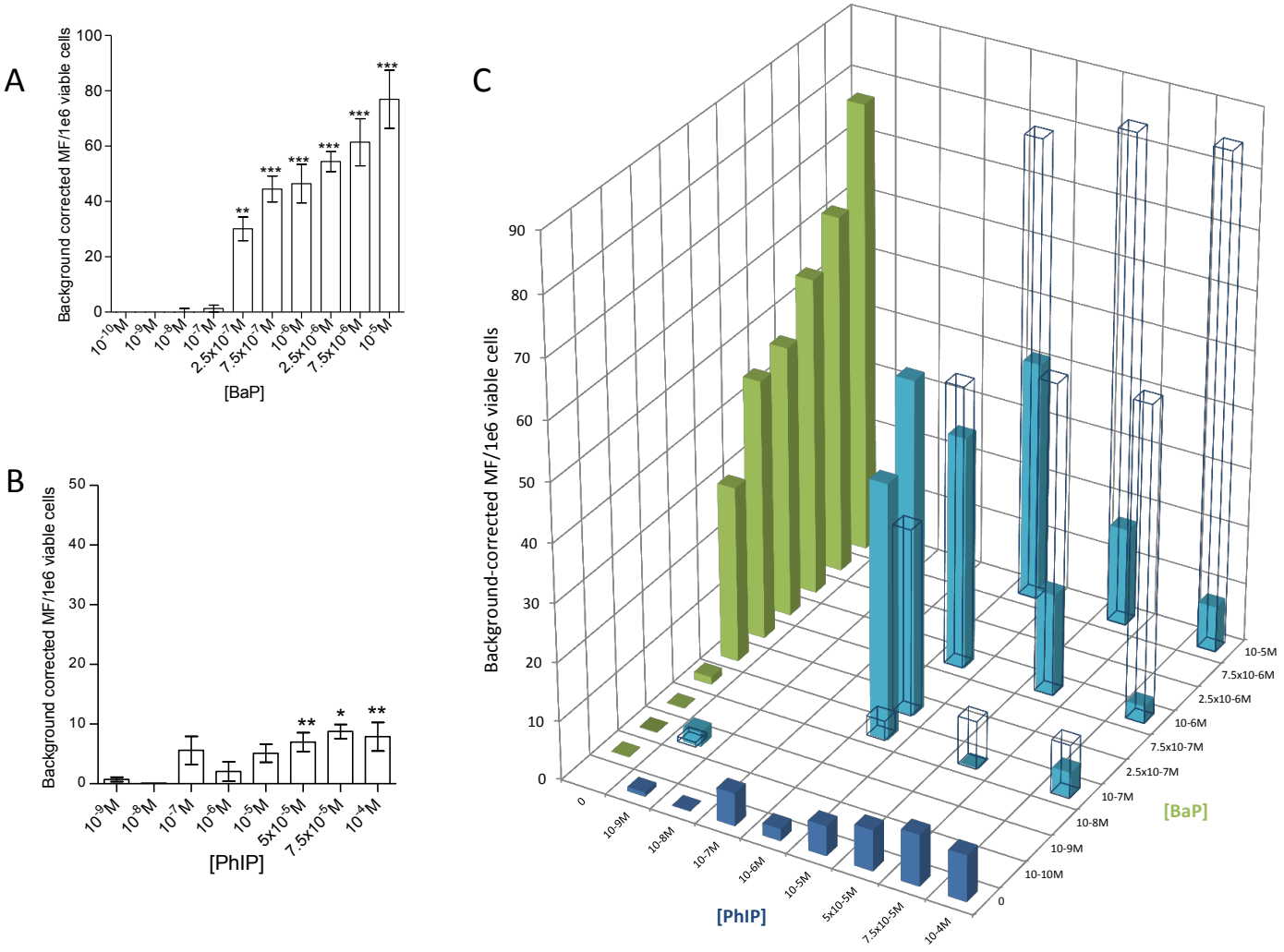

Environ Health Perspect DOI: 10.1289/ehp.1409557
Advance Publication: Not Copyedited

Figure 2.

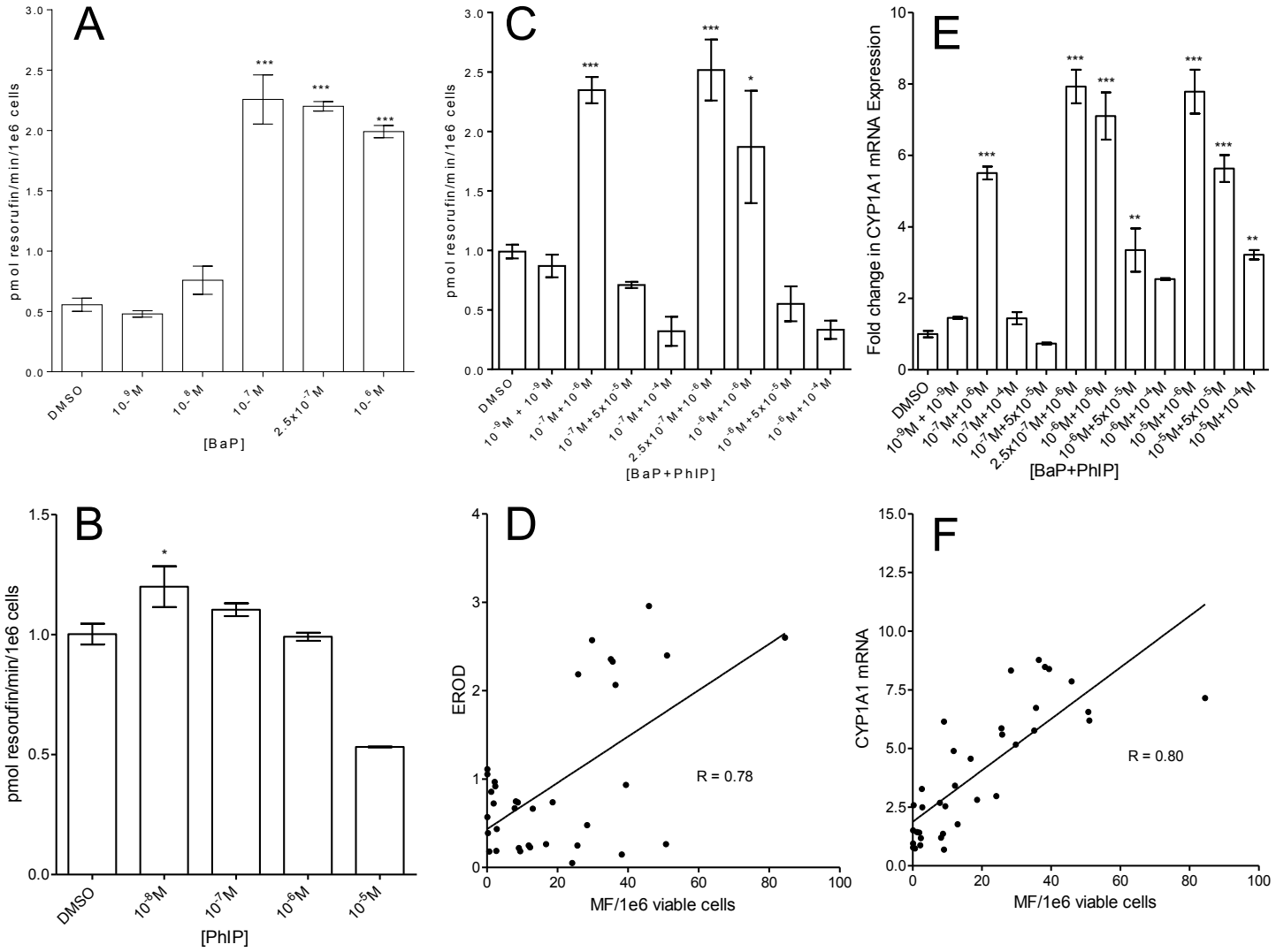

Figure 3.

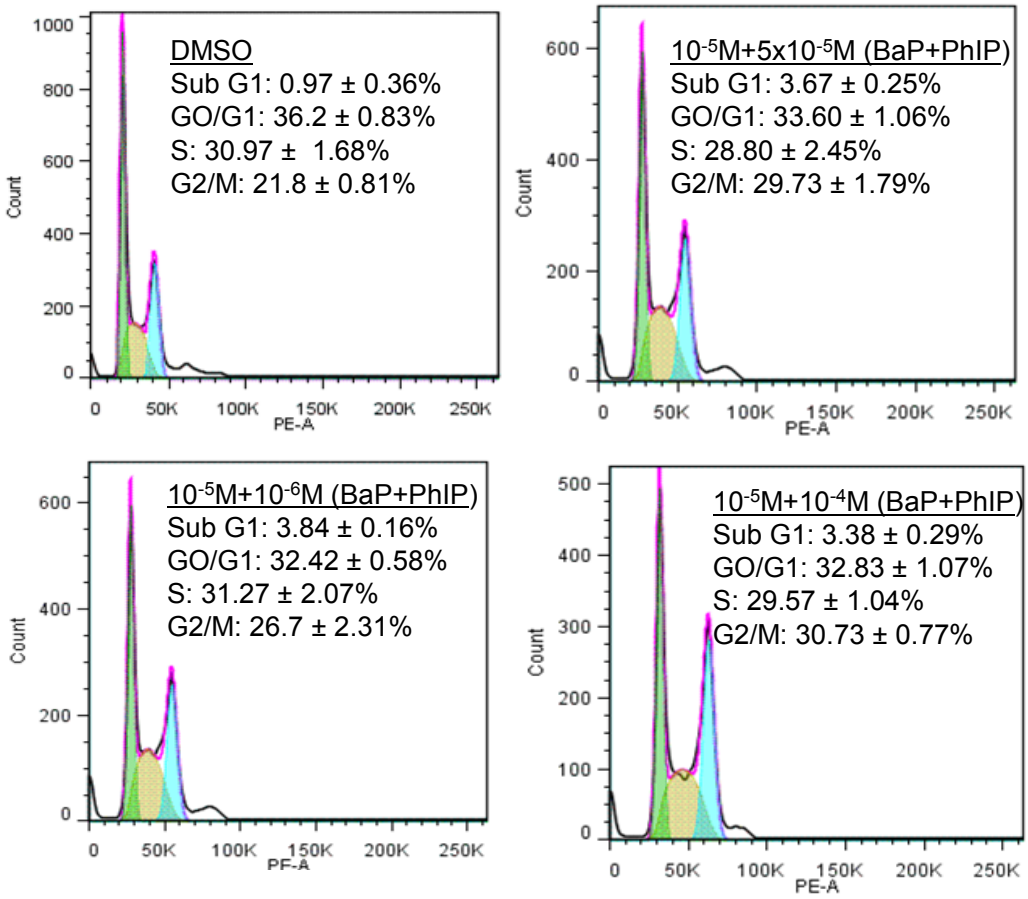
DMSO
Sub G1: 0.97 ± 0.36%
GO/G1: 36.2 ± 0.83%
S: 30.97 ± 1.68%
G2/M: 21.8 ± 0.81%
10-5M+5x10-5M (BaP+PhIP)
Sub G1: 3.67 ± 0.25%
GO/G1: 33.60 ± 1.06%
S: 28.80 ± 2.45%
G2/M: 29.73 ± 1.79%
10-5M+10-6M (BaP+PhIP)
Sub G1: 3.84 ± 0.16%
GO/G1: 32.42 ± 0.58%
S: 31.27 ± 2.07%
G2/M: 26.7 ± 2.31%
10-5M+10-4M (BaP+PhIP)
Sub G1: 3.38 ± 0.29%
GO/G1: 32.83 ± 1.07%
S: 29.57 ± 1.04%
G2/M: 30.73 ± 0.77%
Count
PE-A
0
50K
100K
150K
200K
250K

Environ Health Perspect DOI: 10.1289/ehp.1409557
Advance Publication: Not Copyedited

Figure 4.